JOURNAL OF CATALYSIS 48, 269–283 (1977)

The CO Oxidation Reaction on the Ir(111) Surface

V. P. IVANOV, G. K. BORESKOV, AND V. I. SAVCHENKO

Institute of Catalysis, Novosibirsk, USSR

AND

W. F. EGELHOFF, JR., AND W. H. WEINBERG[1]

Division of Chemistry and Chemical Engineering, California Institute of Technology, Pasadena, California 91125

Received September 30, 1976; revised March 24, 1977

Carbon monoxide oxidation over the (111)iridium surface was found to obey a Langmuir–Hinshelwood reaction rate expression indicative of a surface reaction between a chemisorbed carbon monoxide molecule and a chemisorbed oxygen atom. An extremely small value of the preexponential factor of the rate coefficient (approximately 10^{-11} cm²/sec) was determined, while the activation energy to the surface reaction was found to be 10.5 kcal/mole. The small preexponential factor may well be due to the presence of large, independent islands of each adsorbed reactant on the surface. Since the reaction would be restricted to the region of the boundaries of the islands, this would result in an *apparently* small preexponential factor of the rate coefficient. The primary difference between (111)iridium and various surfaces of platinum and palladium insofar as the reaction between adsorbed oxygen and adsorbed carbon monoxide is concerned is that only at elevated temperatures does the iridium surface exhibit the reaction rates displayed by platinum and palladium at room temperature. Moreover, extensive oxidation of the (111)iridium surface (e.g., 2×10^{-7} Torr oxygen for 10 min at 700°K) was found to induce, under certain conditions, marked changes in the oxidative properties of the surface. These changes are related to the formation of a nonstoichiometric oxide in the near-surface region although the oxygen atoms in this oxide do not participate in the carbon monoxide oxidation reaction.

I. INTRODUCTION

The heterogeneously catalyzed CO oxidation reaction is of considerable interest since its relative simplicity indicates the possibility of a detailed analysis of the reaction mechanism. In response to the opportunities for profitable research in this area, extensive studies have been carried out on the CO oxidation reaction over both Pt (*1*) and Pd (*2*) surfaces. In recent years, the trend of investigation in this field has lead to the application of ultrahigh vacuum (UHV) compatible surface probes such as low-energy electron diffraction (LEED), Auger electron spectroscopy, thermal desorption mass spectrometry, contact potential difference measurements, and both uv- and x-ray photoelectron spectroscopy (*1*, *2*). However, much less attention has been devoted to the CO oxidation reaction over the other Group VIII transition metals in spite of their known similarity to Pt and Pd as heterogeneous catalysts (*3*). In particular, we know of only three previous studies of the CO oxidation

[1] Alfred P. Sloan Foundation Fellow to whom inquiries concerning this paper should be sent.

ISSN 0021-9517

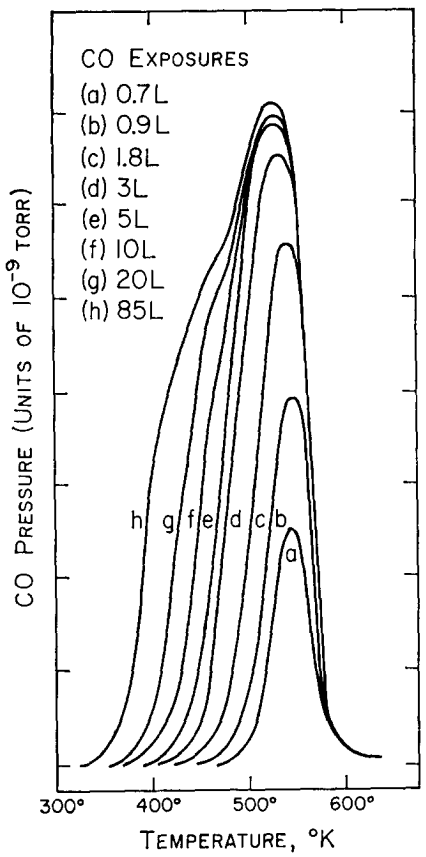

FIG. 1. The thermal desorption spectra of CO following exposures of the clean Ir(111) surface at 325°K to the indicated fluxes of CO. A Langmuir (L) represents an exposure of 10^{-6} Torr sec, and the heating rate was 5°K/sec.

reaction over Ir surfaces under UHV conditions (*4–6*). These investigations were carried out over a clean, well annealed polycrystalline Ir foil (*4*) [the surface of which evidently consisted largely of (110) oriented microcrystallites (*7*)], over an Ir(110) single crystal (*5*), and over an Ir(111) single crystal (*6*).

This paper represents one part in a series of investigations which we are conducting concerning the oxidation of CO on various crystallographic orientations of monocrystalline Ir (*7–9*). The aim of this work is to understand the effect both of the electronic and the geometric structure of the Ir surface on the reaction and to describe completely the microscopic details of the reaction mechanism.

II. EXPERIMENTAL METHODS

All the experimental results reported herein were obtained making use of a stainless steel, UHV chamber pumped both by a sputter ion pump and a titanium sublimation pump, the effective pumping speed of which was 100–200 liters/sec for most gases. This vacuum chamber was equipped with a Varian three-grid LEED–Auger system (grazing incidence Auger gun), a UHV ion gauge, and a monopole mass spectrometer. After bakeout, the base pressure of the instrument was $\lesssim 2 \times 10^{-10}$ Torr. The Ir(111) crystal (the diameter and thickness of which were 7 and 0.6 mm, respectively) was oriented, cut, and polished by standard procedures as described in Ref. (*8*). The crystal was mounted between two 0.3 mm W wires which were spot welded to opposite edges of the crystal. These wires were heated resistively with currents of up to 20 A, and the crystal heating was a consequence of thermal conduction through the spot welds. The crystal temperature was measured with a Ta–W thermocouple spot welded on an edge of the crystal remote from the heating wires. The thermocouple was calibrated from 295 to 827°K in an external furnace and above 1225°K *in situ* by an optical pyrometer. The measured emf developed across the thermocouple was very nearly a linear function of temperature (to within ± 20°K) above 500°K.

The crystal was cleaned and annealed by standard treatments [described in Ref. (*9*)], which are known to produce a clean and well ordered Ir(111) surface. The clean crystal surface gave a sharp (1 × 1) LEED pattern, and the Auger spectrum of the clean surface was essentially identical to that published previously by Christmann and Ertl (*5*) for a clean Ir(110) surface.

III. RESULTS

In Fig. 1, we illustrate the thermal desorption spectra of CO chemisorbed on (111)Ir. The information that these spectra yield concerning the temperature dependence of the CO coverage is an essential ingredient in a complete understanding of the CO oxidation reaction. These desorption spectra are in complete agreement with those published previously for a different Ir(111) crystal in a different UHV system (*8*).

Since CO is known to be adsorbed associatively on (111)Ir (*8*), the rate of desorption of CO is assumed to be described by the first-order rate expression

$$R_d = \nu[\mathrm{CO}]\exp(-E_d/kT), \qquad (1)$$

where R_d is the rate of desorption, ν is the preexponential factor of the desorption rate coefficient, often referred to as the frequency factor, [CO] is the concentration of CO molecules adsorbed on the Ir (i.e., the fractional surface coverage multiplied by the surface concentration of adsites), and E_d is the activation energy for desorption (*10*). For a constant heating rate (β), the activation energy for desorption (E_d) may be calculated from the peak temperature (T_p) in the thermal desorption spectra by making use of the following expression (*10*):

$$E_d = kT_p[\ln(\nu T_p/\beta) - 3.64]. \qquad (2)$$

This equation assumes the pumping speed in the vacuum chamber is sufficiently high that the pressure of CO is directly proportional to the instantaneous rate of desorption. In our case, a pumping speed of 100 liters/sec in a 40 liter chamber with $\beta = 5$°K/sec is more than sufficient to satisfy this assumption.

The value of ν is commonly assumed to be 1×10^{13} sec^{-1} (*11*). However, we have found that a value of 2.4×10^{14} sec^{-1} is more accurate in the case of CO desorption from Ir(111) since this value reconciles the heat of adsorption of CO on Ir(111) with the activation energy of desorption as determined by thermal desorption (*8*).

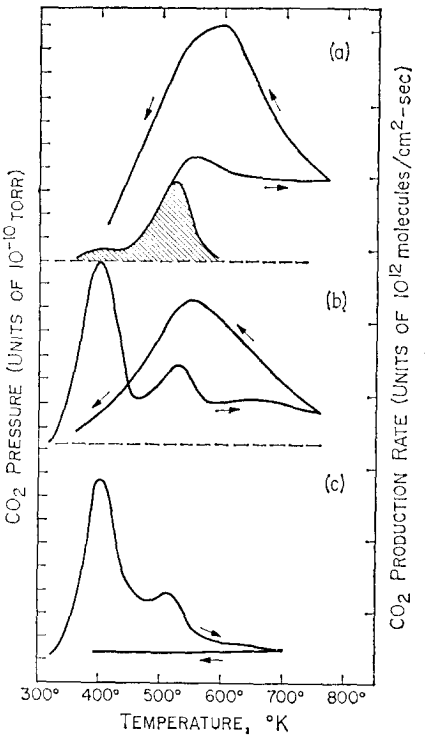

FIG. 2. The CO_2 pressure change and production rate for the CO oxidation reaction on Ir(111) under various conditions. The arrows indicate the direction of temperature change with time. The heating rate was 4°K/sec, and the cooling rate was approximately the same near 500°K. In (a) and (b), the crystal was heated in 8×10^{-8} Torr O_2 and 6×10^{-8} Torr of CO. Prior to (a), the crystal had been heated briefly at 1400°K to produce a clean surface. The shaded area under (a) is the result for heating a CO saturated surface in 8×10^{-8} Torr O_2. Prior to (b), the surface was heavily oxidized at 700°K (see text). Prior to (c), the surface was oxidized as in (b), cooled in O_2 and CO to 325°K, and then heated in vacuum to observe the reaction between coadsorbed CO and oxygen.

In the thermal desorption spectra of Fig. 1, there is a desorption peak at 540°K at very low coverage. The desorption temperature of this peak appears to decrease very slightly with increasing coverage and appears at 525°K when this state reaches saturation. At an exposure which produces

saturation coverage of this binding state, a maximum is observed in the intensity of the $(3^{\frac{1}{2}} \times 3^{\frac{1}{2}})$-$R30°$ LEED pattern (*8*). Using the value $\nu = 2.4 \times 10^{14}$ sec^{-1} and the peak temperature of 525°K, the activation energy for desorption is calculated to be $E_d = 35.9$ kcal/mole. This is in complete agreement with a determination of the activation energy made on a different Ir(111) crystal in a different UHV system (*8*). If we choose $\nu = 1 \times 10^{13}$ sec^{-1}, the activation energy is calculated to be 32.6 kcal/mole.

The LEED pattern for exposures greater than that corresponding to Fig. 1d indicates that the $(3^{\frac{1}{2}} \times 3^{\frac{1}{2}})R30°$ diffraction beams (produced by CO exposures of slightly less than approximately 2.5 L where 1 L ≡ 1 Langmuir ≡ 1×10^{-6} Torr sec) begin to split until, ultimately, a $[2(3)^{\frac{1}{2}} \times 2(3)^{\frac{1}{2}}]$-$R30°$ LEED pattern is observed. This behavior has been interpreted to indicate a continuous compression of the CO overlayer after the coverage exceeds 5.2×10^{14} molecules/cm^2 (*8*). In such a situation, a continuously decreasing value of E_d might be expected so that the skew of Fig. 1f–h at low temperatures is likely to be a manifestation of the loss of registry between the CO and the Ir substrate, as well as repulsive interactions among the adsorbed CO molecules.

In Fig. 1, all exposures of the clean crystal to CO were made with a crystal temperature of approximately 325°K. For the lower exposures to CO ($\epsilon_{CO} < 5$ L), a careful determination was made of the amount of CO to which the crystal was exposed during the cooling to 325°K. The part of this exposure which occurred between 500 and 325°K (generally less than 2×10^{-7} Torr sec) was included in the quoted exposures to ensure accuracy.

In a previous paper (*9*), we have reported results for a study of the chemisorption of oxygen on Ir(111). We shall now recapitulate, briefly, the aspects of that investigation which are of importance in an interpretation of the CO oxidation reaction. There is a coverage-dependent activation energy for desorption of oxygen, the value of which is $E_d \approx (65\text{–}10\theta)$ kcal/mole. Essentially no O_2 desorbs below 800°K. At 300°K, the probability of adsorption of O_2 into a dissociatively chemisorbed state is approximately 0.09, and this value is maintained until saturation coverage is very nearly reached. The activation energy for diffusion of the chemisorbed oxygen adatoms lies between 16 and 19 kcal/mole. It was also found that when the crystal is exposed to approximately 2×10^{-7} Torr of O_2 for several minutes at temperatures above 700°K, an oxide state is formed in the near-surface region. This oxide is quite unreactive with respect to CO in the temperature range in which the oxygen actually adsorbed *on the surface* is highly reactive ($T \geq 400$°K). This oxide state desorbs as molecular O_2 in a single peak at 1270°K.

In the present paper, we consider the influence of this oxide state on the catalytic properties of the Ir(111) surface in the CO oxidation reaction. A similar near-surface oxide apparently forms on the Ir(110) surface, and this will be the subject of another publication (*7*). In Fig. 2, we present results concerning the rate of production of CO_2 as a function of the temperature of the Ir(111) surface under a variety of conditions. In Fig. 2a, the crystal was cleaned and allowed to cool to 325°K in vacuum. A pressure of 6×10^{-8} Torr CO was then admitted to the chamber, and after the surface had become saturated with CO, 8×10^{-8} Torr of O_2 was admitted to the chamber. The Ir crystal was heated, at a constant rate of 4°K/sec, with the indicated CO and O_2 pressure maintained by continuous admission through UHV leak valves. At 775°K, the crystal heating was terminated, and the crystal was allowed to cool in the CO and O_2 ambient. The arrows in Fig. 2 indicate the direction of change of temperature with time. Follow-

ing cooling to 325°K, still in a flow of CO and O_2, the crystal could be heated once again, and an almost identical CO_2 production rate as a function of temperature could be reproduced. When, following such a procedure, the O_2 and CO leak valves were closed with the Ir at 325°K and the crystal heated in a UHV ambient, the thermal desorption spectrum shows three important features. First, the CO desorption (mass 28) spectrum is essentially identical to that shown in Fig. 1g, i.e., the surface is nearly saturated with CO. Second, this desorption spectrum indicates a small amount of O_2 desorption (mass 32) at 1270°K, demonstrating that during the CO oxidation reaction on the initially unoxidized surface, some of the near-surface oxide state is formed. Third, no desorption (or production) of CO_2 (mass 44) was observed, indicating the absence of adsorbed reactive oxygen on the surface following the cooling cycle shown in Fig. 2a. The shaded area under the curve of Fig. 2a represents the CO_2 production rate obtained when, following heating and cooling in O_2 and CO, the CO leak valve was closed after the crystal reached 325°K, and the Ir was then heated in a flow of O_2 only.

The effect on the CO_2 production rate of heavy oxidation of the Ir(111) surface is illustrated in Fig. 2b. The oxidation of the surface was effected by four cycles of heating the crystal to 700°K followed by cooling to 325°K in 2×10^{-7} Torr of O_2. Based on our previous results (*9*), we know that this produces a large concentration of the unreactive, near-surface oxide state. After this heavy oxidation treatment and subsequent cooling to 325°K, 6×10^{-8} Torr of CO was admitted, and the O_2 pressure was adjusted to 8×10^{-8} Torr. At this point, the Ir is covered by oxygen atoms and CO molecules that are adsorbed on a surface which contains the near-surface oxide. The first time this surface is heated in the flow of CO and O_2, a very large CO_2 peak is produced, similar in size and shape to that shown in Fig. 3a. This is due to the reaction between the CO molecules and the oxygen atoms adsorbed on the Ir surface. Note there is an order of magnitude difference in scale between Fig. 2 and 3. When the crystal is then cooled to 325°K maintaining the flow of CO and O_2, and heated for a second time, the result shown in Fig. 2b is obtained. During subsequent heating and cooling cycles in the flow of CO and O_2, the result of Fig. 2b is reproduced with very little change. By comparing Fig. 2a and b, it is clear from the change in relative magnitude of the peaks that the heavy oxidation of the Ir surface has a marked effect on the catalytic properties of the surface insofar as the transient kinetics of the CO oxidation reaction are concerned.

During the heating cycle of Fig. 2b, there are two prominent peaks in the CO_2 production rate which occur at 400 and at 525°K. It is interesting to note that both of these peaks may be attributed to oxygen and CO which are adsorbed on the surface prior to the heating cycle (i.e., subsequent to the cooling cycle of Fig. 2b). This is demonstrated by the results shown in Fig. 2c. These results were obtained by closing both the CO and O_2 leak valves after cooling the Ir to 325°K (as, for example, in Fig. 2b). In Fig. 2c, the crystal was heated in a UHV ambient. That the 525°K peak of Fig. 2b correlates with the 510°K peak of Fig. 2c is supported by the fact that at surface temperatures above 500°K, CO is desorbing rapidly from the Ir. This effect would be expected to decrease the intensity on the high temperature side of the 525°K peak of Fig. 2b and should be manifested as a shift of this peak to a lower temperature as observed in Fig. 2c. These results will be considered further in the next section.

In Fig. 3, we present results for the oxidation of CO by oxygen preadsorbed at saturation coverage, i.e., with no O_2 present

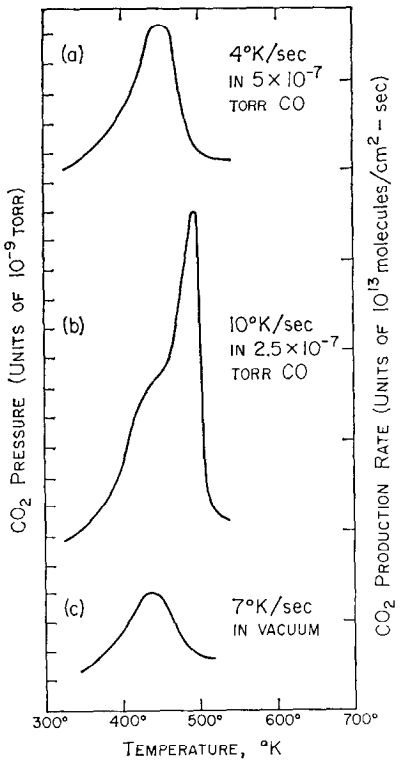

FIG. 3. The CO_2 pressure change and the production rate for the CO oxidation reaction are presented in (a) and (b) for the titration by CO of an Ir(111) surface saturated with oxygen at 325°K. In (c), the surface was exposed first to 20×10^{-6} Torr sec of O_2, then to 20×10^{-6} Torr sec of CO and heated in vacuum to observe the reaction between co-adsorbed oxygen and CO.

in the gas phase. These results were obtained on a surface which contained the near-surface oxide (which can only be removed by high temperature treatment, e.g., 1270°K). However, it was found that whether the near-surface oxide is present or not does not significantly alter the characteristics of the oxidation of CO by oxygen pre-adsorbed at saturation coverage. The importance of the near-surface oxide is clearly seen under the conditions of Fig. 2, which always results in a low concentration of adsorbed oxygen and gives lower rates of CO_2 production than under the conditions of Fig. 3. The results of Fig. 3a are indicative of a surface which was saturated (20×10^{-6} Torr sec) with oxygen at 325°K. A pressure of 5×10^{-7} Torr CO was admitted to the chamber, and the crystal was heated (in the flow of CO) at a rate of 4°K/sec.

It was found that the shape of such curves, which may be thought of as CO titration experiments was affected by the heating rate and the CO pressure. In Fig. 3b, we present the result for titrating the oxygen saturated surface with 2.5×10^{-7} Torr CO and a 10°K/sec heating rate. Figure 3b exhibits a pronounced shoulder and a sharp cutoff in CO_2 production as the reactive oxygen is depleted. These effects are due to a relatively low CO pressure and a relatively high heating rate. For example, a 10°K/sec heating rate and a CO pressure of 8×10^{-7} Torr resulted in a CO_2 pressure curve without the shoulder of Fig. 3b and with the sharp cutoff temperature decreased by about 8°K.

The purpose of Fig. 3c is to illustrate that part of the CO_2 production rate in Fig. 3a and b results from CO already adsorbed on the Ir prior to the initiation of the heating. The curve shown in Fig. 3c was produced by exposing the surface at 325°K to 20×10^{-6} Torr sec of O_2 and 20×10^{-6} Torr sec of CO in that order. Larger exposures of either gas had very little effect on the curve of Fig. 3c. The crystal was then heated in a UHV ambient to produce the result of Fig. 3c. In this case, the CO_2 produced necessarily came from pre-adsorbed oxygen and CO. This procedure was sufficient to remove about half of the adsorbed reactive oxygen. These results are discussed in the next section.

In Fig. 4, the solid line is a representation of the logarithm of the ratio of the measured CO_2 pressure at various temperatures, $P_{CO_2}(T)$, to the measured CO_2 pressure at 350°K plotted against reciprocal temperature for the data of Fig. 3a. For the temperature range 350–450°K, this plot is nearly linear, and the slope may be used to calculate an *apparent* activation energy of 8.4 kcal/mole. However, this is evidently

an oversimplified approach to determining the actual activation energy of the reaction. Figure 3c may be taken to imply that in this temperature range the reaction occurs between adsorbed oxygen and adsorbed CO. Thus, it is reasonable to assume that a Langmuir–Hinshelwood reaction rate expression may apply (a manifestation of a chemical reaction between an adsorbed CO molecule and an adsorbed oxygen atom producing CO_2), i.e.,

$$\alpha P_{CO_2} = R = [CO][O]k^0 \exp(-E_a/kT), \quad (3)$$

where [CO] and [O] are the concentrations of adsorbed CO and adsorbed oxygen, respectively, k^0 is the preexponential factor of the reaction rate coefficient, E_a is the activation energy to the chemical reaction, R is the reaction rate expressed in units of molecules of CO_2 formed per square centimeter of surface per second, P_{CO_2} is the measured CO_2 partial pressure, and α is a proportionality factor determined by the pumping speed of the vacuum chamber for CO_2. When applying this rate expression, it is necessary to correct for the variation in surface coverage both of CO and oxygen as a function of temperature. Prior to an explicit discussion of how this is done, we rewrite Eq. (3) in the following way

$$\ln\left(\frac{P_{CO_2}}{P^0_{CO_2}}\right) - \ln\left(\frac{[CO]}{[CO_0]}\right) - \ln\left(\frac{[O]}{[O]_0}\right) = \frac{E_a}{k}\left(\frac{1}{T_0} - \frac{1}{T}\right), \quad (4)$$

where the superscript zero associated with P_{CO_2} and the subscript zeros associated with the concentrations of CO and oxygen refer to the values at $T_0 = 350$°K. Here, it has been assumed that k^0 is a sufficiently weak function of temperature that the logarithm of the ratio of k^0 at any temperature between 350 and 500°K to the value of k^0 at 350°K is approximately zero.

Making the appropriate correction for the variation in surface oxygen concentration is a straightforward enterprise. In Fig. 3a, all of the reactive oxygen has been removed by 550°K. This is reflected by the fact that subsequent cooling to 325°K followed by heating in 5×10^{-7} Torr CO produces no detectable CO_2. Therefore, the area under the peak in Fig. 3a gives a direct measure of the relative oxygen coverage.

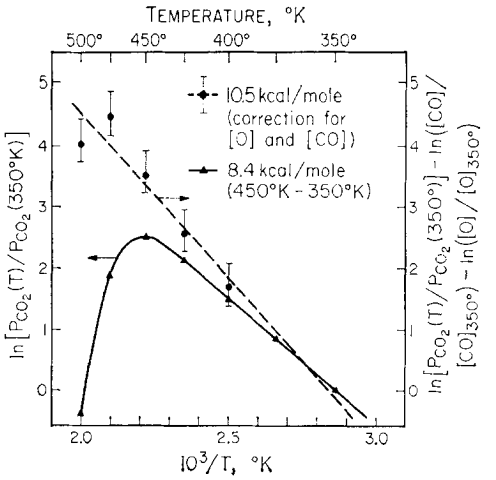

FIG. 4. The left ordinate (▲—) corresponds to a plot of the logarithm of the relative pressure in Fig. 3a. If interpreted as an Arrhenius plot between 350 and 450°K, this gives an activation energy of 8.4 kcal/mole. The right ordinate [(▲) at 350 and 375°K, and (●- - -)] corresponds to a plot of the Langmuir–Hinshelwood reaction rate expression (i.e., taking into account the varying surface concentrations of the reacting species; see text). This demonstrates that the correct activation energy is 10.5 kcal/mole.

The determination of the relative CO surface concentration is somewhat more difficult. However, we can estimate that it must be between 25 and 50% of the saturation coverage value for CO over the entire data range shown in Fig. 3a. We know from previous work that at 325°K, the saturation coverage of CO is 9.1×10^{14} molecules/cm^2, while for oxygen it is 7.9×10^{14} atoms/cm^2 (*8*, *9*). The data in Fig. 3c indicate that just prior to the initiation of the heating in Fig. 3a, the CO coverage must be at least 4×10^{14} molecules/cm^2. From the data in Fig. 1 and

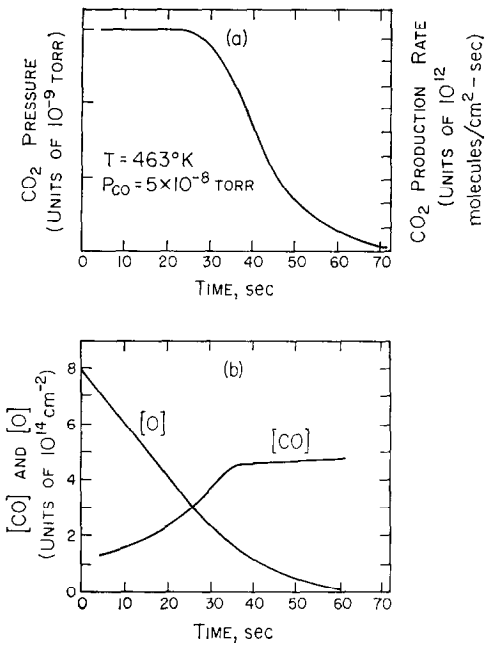

FIG. 5. The CO_2 pressure change and production rate as a function of time is presented in (a) for the titration of an oxygen covered Ir(111) surface by CO at a constant temperature of 463°K. The calculated concentrations of adsorbed CO and atomic oxygen are presented in (b) as a function of time for the titration in (a). The oxygen concentration is calculated simply by graphical integration of (a). See the text for the method of calculating the CO concentration.

the conclusions drawn therefrom, we can estimate that at 500°K in Fig. 3a the coverage of CO will be greater than 2×10^{14} molecules/cm^2 if the sticking probability is no less than 0.5 at this coverage. Both the data in Fig. 1 and previously published results indicate that this is true (*8*). An upper limit on the surface coverage of CO at 500°K in Fig. 3a may be calculated by assuming a sticking probability of unity and using the data of Fig. 1. This upper limit is found to be 4×10^{14} CO molecules/cm^2.

During the course of the reaction, the rate of CO molecules incident upon the crystal is always at least an order of magnitude greater than the CO_2 production rate. Thus, we feel confident that the CO coverage remains between 25 and 50% of its saturation value at 325°K (9.1×10^{14} molecules/cm^2). This range of CO coverage has been included in constructing the broken line of Fig. 4 (as error bars on the points). The solid circles in Fig. 4 represent the data which have been corrected for the variation in the surface oxygen concentration. The broken line drawn through the corrected points (the 350 and 375°K points did not require correction for varying [O]) gives a much better estimate of the actual activation energy for the surface reaction. As indicated in Fig. 4, the slope of this broken line yields an activation energy of 10.5 kcal/mole.

Using our estimates of the surface coverages of CO and oxygen, the measured rate of production of CO_2, and the activation energy, we make use of Eq. (3) in order to determine k^0, the preexponential factor of the reaction rate coefficient. This yields a value for k^0 of 1×10^{-11} cm^2/sec which is reliable to within approximately an order of magnitude. Sources of error in this determination are several. For example, the area under the curve in Fig. 3a implies an initial oxygen coverage of only 3.4×10^{14} atoms/cm^2. This is probably indicative of an error of as much as 50% in either the ion gauge or in the measured value of the CO_2 pumping speed. Either of these, or some combination of both, is plausible in experimental work of this type. An even more important source of uncertainty in the preexponential factor results from uncertainties in the activation energy. An error of 2 or 3 kcal in the determination of the latter implies an uncertainty of on the order of an order of magnitude in k^0.

In Fig. 5a, we present the data for a CO titration experiment very similar to that shown in Fig. 3a. The difference is that in Fig. 5a the crystal temperature was held at a constant value of 463°K. The experimental results of Fig. 5a were obtained in the following way. The surface was exposed to 20×10^{-6} Torr sec of O_2 at 325°K and

then heated to 463°K. A pressure of 5×10^{-8} Torr CO was admitted to the chamber, and the CO_2 pressure was monitored as a function of time. The zero of time in Fig. 5 corresponds to the point at which CO is admitted to the vacuum chamber. The CO and CO_2 pressures stabilized in less than 3 sec under the quoted conditions.

In Fig. 5b, we present the calculated CO and oxygen surface coverages as a function of time corresponding to the experimental conditions of Fig. 5a. The oxygen coverage is determined by a graphical integration of Fig. 5a together with the known value for saturation coverage of oxygen on the surface. The CO surface coverage is somewhat difficult to determine. However, a reasonable estimate may be obtained in the following way. We assume that the data shown in Fig. 5a may be described by Eq. (3). In the application of Eq. (3), we use known values for the rate of production of CO_2 taken from Fig. 5a, we assume that the preexponential factor of the reaction rate coefficient, k^0, is independent of time, we calculate the Boltzmann factor using an activation energy of 10.5 kcal/mole, and we use known values of the surface oxygen concentration taken from Fig. 5a. We may now estimate the surface coverage of CO as a function of time without making any assumption concerning k^0 (other than that it is time independent) if we know the surface CO concentration at one particular point in time. We choose to ascertain the surface concentration after the reaction time has reached 50 sec. This is accomplished in the following way. The rate of impingement of CO on the Ir surface is 1.8×10^{13} molecules/cm^2 sec. The oxygen concentration on the surface after the reaction has proceeded for 50 sec is approximately 5×10^{13} atoms/cm^2, and the corresponding production rate of CO_2 is 2×10^{12} molecules/cm^2 sec. These values, even if in error by as much as a factor of 2, together with the CO desorption data of Fig. 1, indicate that the CO concentration at the 50 sec mark in the reaction is essentially equal to the equilibrium coverage value at a pressure of 5×10^{-8} Torr and a temperature of 463°K. The change in the activation energy for desorption as a function of CO coverage (based on Fig. 1) ensures that at the 50 sec mark, the CO concentration will be approximately 4.5×10^{14} molecules/cm^2. This value is certainly correct to within a factor of 2. Using this derived value of the CO coverage, we now use Eq. (3) to determine the CO surface coverage as a function of time during the course of the reaction. The result is presented in Fig. 5b.

As emphasized earlier, the calculation of the surface CO concentration after the reaction had proceeded for 50 sec did not require *a priori* knowledge of k^0. However, once this surface coverage was independently derived then the value of k^0 was uniquely determined. The value of k^0 so determined is 2×10^{-11} cm^2/sec, and this was then used in the subsequent calculation of [CO] as a function of time, i.e., the result presented in Fig. 5b. This value of k^0 is in good agreement with that previously deduced from the data shown in Fig. 4, namely, 1×10^{-11} cm^2/sec.

IV. DISCUSSION

The results of Fig. 2 illustrate the changes in the catalytic properties of the Ir(111) surface following heavy oxidation. The complexity of these results prevents a complete microscopic interpretation of the reaction mechanism. However, a number of useful insights of a more general nature may be obtained.

In Fig. 2a, during the heating cycle the increase in the rate of CO_2 production is evidently due to the desorption of CO providing areas of clean surface on which oxygen can adsorb and subsequently react. This behavior is completely consistent with a large body of previous work on various Pt (*1*) and Pd (*2*) surfaces. The

decrease in the rate of CO_2 production which appears during the heating cycle in Fig. 2a near 550°K has also been observed previously in the case of CO oxidation over Pt (*1*) and Pd (*2*). This decrease in the rate is almost certainly related to the rapidly decreasing equilibrium coverage of CO in this temperature regime as demonstrated in Fig. 1. The desorption of O_2 does not begin until 800°K. The fact that the rate of CO_2 production does not decrease so rapidly as the equilibrium coverage of CO is easily understood. There are two opposing effects occurring. The Boltzmann factor in the Langmuir–Hinshelwood reaction rate expression increases rapidly with increasing temperature partially offsetting the decrease in the equilibrium coverage of CO.

It is rather surprising that during the cooling cycle in Fig. 2a, the rate of production of CO_2 increases so dramatically. At a temperature above 550°K in this pressure range and with a heating (and cooling) rate of only 4°K/sec, ample time would certainly be expected to have elapsed for equilibrium to have been established. However, above approximately 550°K in Fig. 2a, a slowly increasing temperature gives a quite different CO_2 production rate than a slowly decreasing temperature. The fact that the data shown in Fig. 2a are completely reproducible indicates that in this regime the surface reaction is more complicated than might be expected.

The shaded area under Fig. 2a has a very straightforward interpretation. At 325°K when the surface is saturated with CO, no reaction with gas phase O_2 can occur. Indeed, no oxygen can adsorb on the surface when it is saturated with CO. When the Ir is heated in 8×10^{-8} Torr O_2, oxygen can adsorb and react to form CO_2 as the CO begins to desorb. As the temperature increases, the adsorbed CO is depleted. Since there is essentially no CO in the gas phase, the rate of production of CO_2 approaches zero with decreasing concentration of adsorbed CO.

The results shown in Fig. 2b indicate that the heavy oxidation of the Ir surface causes significant changes in the character of the rate of CO_2 production as manifest by the charge in the relative peak heights during the heating cycle. The fact that Fig. 2b is reproducible during *repeated* heating and cooling cycles in the presence of gas phase CO and O_2 indicates that this change in catalytic activity of the surface is not a temporary aberration but rather a permanent change. Of course, the original catalytic properties of the Ir surface (as in Fig. 2a) may be restored by decomposing the near-surface oxide by means of a high temperature (i.e., $\gtrsim$1270°K) treatment of the crystal.

The results of Fig. 2c indicate that this apparent change in catalytic activity, produced by the heavy oxidation of the surface, takes the form of altering the concentration both of adsorbed CO and adsorbed oxygen following the cooling cycle of Fig. 2b to 325°K. At 325°K in Fig. 2b, both reactive oxygen and CO are adsorbed. In contrast, in Fig. 2a at 325°K, essentially no reactive oxygen is present at the surface. Therefore, the heavy oxidation of the surface has made it possible for the crystal to cool to 325°K in the presence of gaseous CO and O_2 and have an appreciable amount of reactive oxygen adsorbed as the temperature becomes low enough so that the reaction rate between adsorbed CO and oxygen is negligible. In Fig. 2b, at 400°K the rate of CO_2 production is much larger for the heating cycle than the cooling cycle. This is not difficult to understand since at 400°K the heating rate is greater than the cooling rate. The amplitude of the 400°K peak in the heating cycle depends on the magnitude of the heating rate.

The data in Fig. 3 provide a number of interesting insights into the mechanism of the CO oxidation reaction over (111) Ir. The production of CO_2 indicated in Fig. 3c is due to a surface reaction between adsorbed CO and adsorbed oxygen since

the Ir(111) surface with pre-adsorbed CO and oxygen was heated in an UHV ambient. This shows that, at least below 450°K, the CO_2 production in Fig. 3a and b is also due to a surface reaction between a CO admolecule and an oxygen adatom. This type of surface reaction is generally referred to as one which obeys Langmuir–Hinshelwood kinetics. The production rate of CO_2 decreases more rapidly above 450°K for the data shown in Fig. 3c compared to that shown in Fig. 3a and b. This is due partly to desorption of CO from the surface but mainly to depletion of CO which is consumed in the oxidation reaction. In the case of the data shown in Fig. 3a and b, the presence of CO in the gas phase will maintain an appreciable concentration of adsorbed CO thereby permitting the Langmuir–Hinshelwood reaction to continue until all the reactive oxygen is removed from the surface.

The shoulder at 435°K in Fig. 3b and its absence in Fig. 3a reflect the effect of lowering the CO pressure and increasing the heating rate. In the case of the more rapid heating rate at the lower CO ambient pressure, as in Fig. 3b, the CO is reacted away from the surface via the oxidation reaction at a more rapid rate than it is replenished from the gas phase. This means that the shoulder at 435°K in Fig. 3b is analogous to the peak in Fig. 3c, i.e., the maximum in the rate of CO_2 produced by CO and oxygen which were adsorbed prior to the initiation of the heating. The peak which occurs at 495°K in Fig. 3b is thus due to a reaction between pre-adsorbed oxygen and CO which is adsorbed during the heating of the Ir. As discussed in the previous section, when the analogous titration experiment indicated in Fig. 3b is performed with an ambient of 8×10^{-7} Torr CO, an increase in the rate of CO_2 production is observed with no hint of a low temperature shoulder, and the temperature of the peak and sharp cutoff are lowered by 8°K. This indicates that the larger ambient pressure of CO is sufficient to maintain a surface coverage of CO near its maximum value (compatible with the coverage of co-adsorbed oxygen). This also indicates that a depletion of adsorbed CO in Fig. 3b above 450°K causes a shift to higher temperatures in the maximum value of the CO_2 production rate. The probable reason for this is that the reaction of adsorbed oxygen goes to completion more slowly if the concentration of adsorbed CO is less than the saturation value compatible with the amount of co-adsorbed oxygen.

The results in Fig. 4 prove that when the variation in oxygen surface coverage is taken into account, the data in Fig. 3a are in good agreement with a Langmuir–Hinshelwood rate expression. However, since the concentration of adsorbed CO and the CO pressure are undergoing only very small changes with temperature in Fig. 3a, the construction indicated in Fig. 4 would also be in good agreement with an impact, or Eley–Rideal, mechanism. The Eley–Rideal rate expression is

$$R_{CO_2} = k^0[O]\frac{P_{CO}}{(2\pi MkT)^{\frac{1}{2}}} \exp(-E_a/kT), \quad (5)$$

where P_{CO} is the CO partial pressure, M is the molecular weight of CO, and the other symbols have the same meaning as in Eq. (3). The reason the plot in Fig. 4 also agrees with the Eley–Rideal rate expression is that both $\ln([CO]/[CO]_0)$ and $\ln(P_{CO}/P^0{}_{CO})$ are approximately zero for the data of Fig. 3a. Although the construction of Fig. 4 does not *uniquely* distinguish between the two possible mechanisms, it does give a valid measure of the activation energy for the reaction. The slope of the broken line in Fig. 4 (i.e., after correction for the variation in oxygen surface coverage) yields a value of 10.5 kcal/mole for the activation energy of the oxidation reaction over (111)Ir. The slope of the linear part

of the solid line in Fig. 4 which is uncorrected for the variation in reactant coverages with temperature indicates that an Arrhenius plot of the CO_2 production rate yields an erroneous value for the activation energy. This is a strong, yet sometimes unappreciated, argument for including the effect of variations in surface coverages with temperature when determining the activation energy of a surface catalyzed reaction. Our value of 10.5 kcal/mole for the activation energy is in agreement with the work of Küppers and Plagge (*6*) who estimated it to be less than 20 kcal/mole.

One of the most important implications of our isothermal titration experiments, the results of which are illustrated in Fig. 5a, is that the oxidation reaction does not proceed via a CO impact mechanism. An impact mechanism is often referred to in the catalysis literature as one which obeys an Eley–Rideal rate expression. However, the designation "Eley–Rideal mechanism" is generally used loosely to describe any surface reaction where the surface concentration of one of the reacting species is rather small even though its partial pressure in the gas phase may be relatively large. It seems to us highly probable that many catalytic reactions which are said to obey Eley–Rideal kinetics are in no way describable by an impact mechanism at the molecular level. Rather, many of these reactions undoubtedly require adsorption of the reactant as an initial step, even if the lifetime of the adsorbed state is quite short (e.g., of order a nanosecond to a millisecond). It should be recalled that a nanosecond is six to seven orders of magnitude *longer* than the time required for a typical electronic structural rearrangement. Any reaction in which both reactants exist on the surface in adsorbed states prior to reaction should properly be described by a rate equation written in terms of adsorbed concentrations, for example, the Langmuir–Hinshelwood rate expression given in Eq. (3). By an impact mechanism, we mean a reaction in which one gas phase reactant is incident upon another adsorbed reactant, and the product molecule is formed in one concerted motion. For example, in the oxidation of CO, the Eley–Rideal or impact reaction scheme, described by Eq. (5), would require that the chemical bond between an adsorbed oxygen atom and the substrate is being broken as a bond between the oxygen adatom and the carbon atom in a CO molecule is simultaneously being formed. This concerted bond scission and formation occurs between the oxygen adatom and a CO molecule *which is not adsorbed on the substrate.* The impact, or Eley–Rideal, mechanism of Eq. (5) is not a valid description of our results for CO oxidation over (111)Ir. This may be seen quite clearly from the results shown in Fig. 5a since the rate of CO_2 production does not vary directly with the concentration of adsorbed oxygen, the latter of which is indicated in Fig. 5b. Nevertheless, it might be suggested that the rate of production of CO_2 is constant for the first 30 sec of the reaction, as in Fig. 5a, due to an impact mechanism in which the cross section for reaction between incident CO molecules and oxygen adatoms is sufficiently large that the reaction probability per incident CO does not decrease below its initial value at saturation coverage of oxygen until the oxygen coverage is less than 3×10^{14} atoms/cm^2. However, Fig. 5a indicates an initial reaction probability of approximately unity (one CO_2 molecule produced per incident CO molecule). Such a large reaction probability would certainly be reasonable only in the limit of a vanishingly small activation energy. The reason for this is that for the impact mechanism to be operative, the energy necessary to surmount any activation barrier would have to be localized at the oxygen atom on which the CO molecule is incident or else present in the incident CO molecule. The time interval of the actual impact (10^{-13} sec) is simply too short for substantial energy redistribution

to occur. However, there is clearly an activation energy to this reaction as Fig. 4 indicates. This conclusion is substantiated by the fact that the (2 × 2) LEED pattern which is observed upon chemisorption of oxygen on (111)Ir is unaffected by CO exposures of 100×10^{-6} Torr sec at a crystal temperature of 325°K.

The incompatibility of an impact mechanism which proceeds with nearly unity probability and an appreciable activation energy barrier (compared to kT) for that process can perhaps be illustrated more clearly by considering numerical values of the reaction cross section. If we assume an activation energy of 10.5 kcal/mole, we may use the Boltzmann distribution to calculate that at 463°K only 1.2×10^{-5} of the oxygen–iridium complexes will be in an activated state 10.5 kcal/mole or more above the ground state. There is, of course, no assurance that there exists an excitation of the oxygen–metal system which would induce a reaction with an incident CO molecule. However, even if there is such an excitation, only 1.2×10^{-5} of the oxygen atoms can be in that state at 463°K. Thus, we conclude that the incident CO would have to impact upon a very large number of oxygen atoms simultaneously in order to exhibit a reaction probability of unity via an impact mechanism. With an oxygen saturation coverage on Ir(111) of 7.9×10^{14} atoms/cm^2, this implies a reaction cross section of 1×10^6 Å^2. Certainly, a CO molecule with a Van der Waals radius of approximately 2.5 Å cannot interact simultaneously with all oxygen atoms present in a circular area on the surface, the diameter of which is greater than a 1000 Å. Thus, we conclude that in the CO oxidation reaction, if there is a significant activation energy (compared to kT), the reaction rate can only approach 1 CO_2 molecule formed/incident CO molecule if the CO passes through an intermediate adsorbed state. An important question for future studies to resolve is how strongly the CO is bound to the surface in this adsorbed state. In the results in Fig. 3, the CO is certainly chemisorbed. However, there might well be some reaction conditions where a physically adsorbed CO molecule plays the role of the intermediate.

The preexponential factor of the reaction rate coefficient of Eq. (3) was calculated from the data shown in Figs. 4 and 5 and was found to be approximately 10^{-11} cm^2/sec. This is an extremely small value for a rate coefficient which describes a reaction between two adsorbed species. A more typical value would be 10^{-2} cm^2/sec (*11*). This leads us to propose that either the oxygen or the CO (or both) is adsorbed in a mutually exclusive island structure, and the reaction between them occurs only at the boundaries of the islands. Support for this suggestion comes from our observation of superimposed LEED patterns indicative both of adsorbed CO [a$(3^{\frac{1}{2}} \times 3^{\frac{1}{2}})R30°$ structure] and adsorbed oxygen [a (2 × 2) structure] upon coadsorption of CO and O_2 (*12*). This suggests that both the CO and O_2 form *separate* island domains on the (111)Ir surface, and the characteristic dimension of each island is *at least* 100 Å, the coherence width of the incident electron beam used in the LEED experiments. This island formation has the effect of limiting the fraction of the adsorbed species which can participate in the reaction. However, the discrepancy between the measured value of 10^{-11} cm^2/sec and the expected value of 10^{-2} cm^2/sec is nine orders of magnitude. This implies that the average island diameter is on the order of a distance corresponding to 10^4 close-packed adatoms or molecules. Since this is evidently quite a large island size, it may well be that additional, and as yet unknown, phenomena also contribute to this very small preexponential factor of the oxidation reaction rate coefficient.

Two additional possible reasons for the small observed preexponential factor are suggested from an activated complex

formulation of the Langmuir–Hinshelwood rate expression (*13*). One possibility is an unusually small value for the transmission coefficient, i.e., the probability that once a hypothetical activated complex reaches the saddle point in the relevant potential energy surface, it will then subsequently attain that region of phase space which constitutes the products of the chemical reaction (*14, 15*).

A second possibility is an unusually large negative value for the activation entropy of the reaction. If we consider the preexponential factor of the rate coefficient to be a product of a frequency factor kT/h and an exponential of the activation entropy, we find that a value of approximately -43 cal/mole-°K is necessary for agreement with our experimental data. This implies that the activated complex is considerably less mobile than the reactants, and this suggestion has been offered previously for abnormally small observed preexponential factors in desorption reactions (*16–19*).

An additional possibility is that the activated complex theory point of view is not a valid description of the oxidation reaction of CO on the (111) surface of Ir. As has been discussed previously (*20, 21*), for either extremely strong or extremely weak coupling between the reactants and the substrate, activated complex theory breaks down, and the preexponential factors become very much smaller.

Although it is by no means clear which, if any, of these phenomena (in addition to the presence of independent islands on the surface) is relevant to the CO oxidation reaction on Ir(111), it is interesting that Bonzel and Burton (*1*) in a study of the Langmuir–Hinshelwood reaction between oxygen and CO on Pt (110) reported the reaction rate coefficient to be 1.8×10^{-11} cm²/sec and the activation energy to be 7.9 kcal/mole.

SUMMARY

Our major conclusions may be summarized as follows:

1. Heavy oxidation of the Ir(111) surface (e.g., 700°K in 2×10^{-7} Torr O_2 for 10 min) causes complex changes in the catalytic properties of the surface under certain conditions in the CO oxidation reaction. These changes are associated with the formation of a nonstoichiometric oxide in the near-surface region.

2. All our results indicate that the oxidation reaction proceeds via a Langmuir–Hinshelwood mechanism in which both CO and oxygen are chemisorbed on the (111)Ir before they react. We find no evidence for an Eley–Rideal mechanism (assuming this is defined as an impact mechanism in which a CO molecule incident upon an adsorbed oxygen atom forms a CO_2 molecule without passing through a surface intermediate as adsorbed CO). If the definition of the Eley–Rideal mechanism is extended to include reaction with CO which adsorbs on the surface for even a brief time (e.g., physically adsorbed CO), then the clarity of its microscopic distinction from the Langmuir–Hinshelwood mechanism is obscured.

3. The analysis of our results of titrating (i.e., reacting) oxygen chemisorbed at saturation coverage on an Ir(111) surface with CO, both at constant temperature and with linearly increasing temperature, leads to the same rate expression of the Langmuir–Hinshelwood type, namely,

$$R_{CO} \approx 10^{-11}[CO][O] \times \exp\left(\frac{-10.5 \text{ kcal/mole}}{kT}\right) \text{cm}^{-2}\,\text{sec}^{-1},$$

where R_{CO_2} is the rate of production of CO_2 per square centimeter of Ir(111) per second, and [CO] and [O] are the concentrations of adsorbed molecular CO and atomic oxygen per square centimeter. The activation energy to this reaction is 10.5

kcal/mole, and the preexponential factor of the reaction rate coefficient is 10^{-11} cm^2/sec.

4. The extremely low value of the preexponential factor of the Langmuir–Hinshelwood reaction rate coefficient, 10^{-11} cm^2/sec, is consistent with our LEED observation of the formation of ordered islands containing exclusively chemisorbed CO and oxygen. The value of 10^{-11} cm^2/sec implies that these islands are quite large on (111)Ir, on the order of 10,000 Å in mean diameter.

5. It appears that the essential difference between Ir(111) and various surfaces both of Pt and Pd insofar as CO oxidation catalysis is concerned is that the reaction between adsorbed CO and adsorbed oxygen occurs very rapidly at room temperature both on Pt and Pd, but at the same rate only at slightly elevated temperatures on Ir(111).

ACKNOWLEDGMENT

This work represents one phase of the Joint US–USSR Program in Chemical Catalysis and was supported by the National Science Foundation under Grant No. CHE74-09019.

REFERENCES

1. Langmuir, I., *Trans. Faraday Soc.* **17**, 672 (1922); Heyne, H., and Tompkins, F. C., *Proc. Royal Soc. (London) A* **292**, 460 (1966); Tretyakov, I. I., Sklyarov, A. V., and Shub, B. R., *Kinet. Katal.* **11**, 166 (1970); Palmer, R. L., and Smith, J. N., Jr., *J. Chem. Phys.* **60**, 1453 (1974); Hori, G. K., and Schmidt, L. D., *J. Catal.* **38**, 335 (1975); Bonzel, H. P., and Burton, J. J., *Surface Sci.* **52**, 223 (1975).
2. Ertl, G., and Koch, J., *Z. Phys. Chem. N. F.* **69**, 323 (1970); Ertl, G., and Koch, J., *in* "Adsorption-Desorption Phenomena" (F. Ricca, Ed.), p. 345. Academic Press, London, 1972; Ertl, G., and Koch, J., *Proc. Int. Congr. Catal., 5th* p. 963 (1973); Matsushima, T., and White, J. M., *J. Catal.* **39**, 265 (1975); **40**, 334 (1975); Matsushima, T., Mussett, C. J., and White, J. M., *J. Catal.* **41**, 397 (1976).
3. Emmett, P. H. (Ed.), "Catalysis," Vol. I–VII. Reinhold, New York, 1955.
4. Ageev, N. V., and Ionov, N. I., *Kinet. Katal.* **14**, 687 (1973).
5. Christmann, K., and Ertl, G., *Z. Naturforsch.* **28a**, 1144 (1973).
6. Küppers, J., and Plagge, A., *J. Vac. Sci. Technol.* **13**, 259 (1976).
7. Ivanov, V. P., Savchenko, V. I., Tataurov, V. L., Boreskov, G. K., Egelhoff, W. F., Jr., and Weinberg, W. H., *Dokl. Acad. Nauk, USSR,* in press.
8. Comrie, C. M., and Weinberg, W. H., *J. Vac. Sci. Technol.* **13**, 264 (1976); *J. Chem. Phys.* **64**, 250 (1976).
9. Ivanov, V. P., Boreskov, G. K., Savchenko, V. I., Egelhoff, W. F., Jr., and Weinberg, W. H., *Surface Sci.* **61**, 207 (1976).
10. Redhead, P. A., *Vacuum* **12**, 203 (1962).
11. Schmidt, L. D., *Catal. Rev.* **9**, 115 (1974).
12. Comrie, C. M., Egelhoff, W. F., Jr., and Weinberg, W. H., unpublished data.
13. Weinberg, W. H., *J. Catal.* **28**, 459 (1973).
14. Pétermann, L. A., *in* "Adsorption–Desorption Phenomena" (F. Ricca, Ed.), p. 227. Academic, London, 1972.
15. Jelend, W., and Menzel, D., *Surface Sci.* **42**, 485 (1974).
16. Lapujoulade, J., *Nuovo Cimento Suppl.* **5**, 433 (1967).
17. Goymour, C. G., and King, D. A., *J. Chem. Soc., Faraday I* **68**, 280 (1972).
18. Mazumdar, A. K., and Wassmuth, H. W., *Surface Sci.* **30**, 617 (1972).
19. Menzel, D., *in* "Interactions on Metal Surfaces" (Topics in Applied Physics), (R. Gomer, Ed.), Vol. 4, p. 101. Springer, Berlin, 1975.
20. Kramers, H. A., *Physica* **7**, 284 (1940).
21. Suhl, H., Smith, J. H., and Kumar, P., *Phys. Rev. Lett.* **25**, 1442 (1970).